ISBN: 978-3-95450-208-0 doi:10.18429/JACoW-IPAC2019-WEPTS101

A GENERAL COMPARISON ON IMPEDANCE THEORY AND CST SIMULATION OF DISCONTINUITIES

N. Khosravi, M. Akhyani, E. Ahmadi[1], A. Mashal[1], H. Karimi[2], S. Dastan[3]
Iranian Light Source Facility (ILSF), IPM, Tehran, Iran
[1]also at Iran University of Science and Technology, Tehran, Iran
[2]also at Isfahan University of Technology, Isfahan, Iran
[3]also at Iran University of Guilan, Guilan, Iran

Abstract

Inhomogeneity of vacuum chamber components is the main source of coupling impedance. Nowadays, wake impedances are mostly predictable by 3D codes and analytical prediction of impedance theories can be helpful as a side solution. On the other hand, some asymmetries in the geometry of components might make troubles and lead to imprecise numerical results in 3D simulations. Analytical approximation of discontinuities, holes and grooves can give us an estimation of expected results and can be used as a benchmark in the case that we do not have any experimental data.

To clarify the validity of theoretical expressions, general discontinuities are simulated in CST Particle Studio. The comparison of final results is presented here. At last, Resistive Wall impedance and some general discontinuities of components at ILSF storage ring are compared form the theoretical and simulation point of view.

INTRODUCTION

Pumping holes, resistive walls (RWs) [1], flange gaps [2], beam position monitors (BPM) [3-5], bellows and tapers[6] can be named as the previously designed ILSF storage ring components. Our aim in this report is to compare the simulation results of these components with theoretical models.

This study is categorized in 4 parts:

- Resistive Walls
- Tapers
- Holes
- Rectangular grooves.

COMPONENTS

Resistive Walls

GZZ equation was proposed by *Gluckstern*, *Zeijts* and *Zotter* [7], which can be considered in this configuration [8]

$$\frac{Z_{\parallel}^{RW}(\omega)}{L} = (1+i\,sign\,\omega)\frac{Z_0|\omega|\delta_s(\omega)}{4\pi cb}G_0$$
$$\frac{Z_{\perp}^{RW}(\omega)}{L} = (i+sign\,\omega)\frac{Z_0\delta_s(\omega)}{2\pi b^3}G_{1x,y} \qquad (1)$$

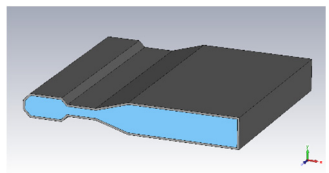

Figure 1: Vacuum Chamber geometry in RW calculations.

The geometry of ILSF vacuum chamber is presented in Figure 1. In Figure 2, we can observe both the analytical evaluation by *GZZ* equation and the simulated impedance for ILSF vacuum chamber resistive wall. In the case of noncircular vacuum chambers, it is normal to approximate the chamber shape by ellipse or rectangle for analytical estimations of the resistive wall. The elliptical and rectangular approximations for ILSF case are shown in Figures 2-4 by green and black colors, respectively.

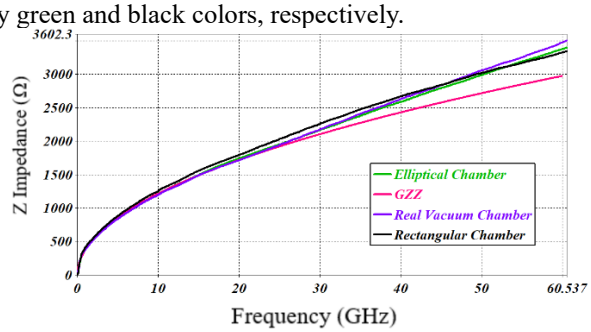

Figure 2: Longitudinal impedance of the resistive wall for Figure 1 geometry (violet), GZZ analytical equation (purple), approximated vacuum chamber in rectangular (black) and elliptical (green) geometries.

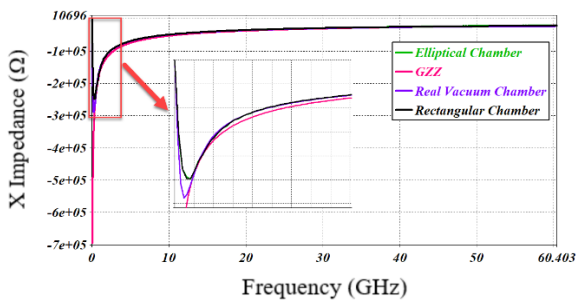

Figure 3: Transverse resistive wall impedance for Figure 1 geometry (violet), GZZ analytical equation (purple), approximated vacuum chamber in rectangular (black) and elliptical (green) geometries.

ISBN: 978-3-95450-208-0 doi:10.18429/JACoW-IPAC2019-WEPTS101

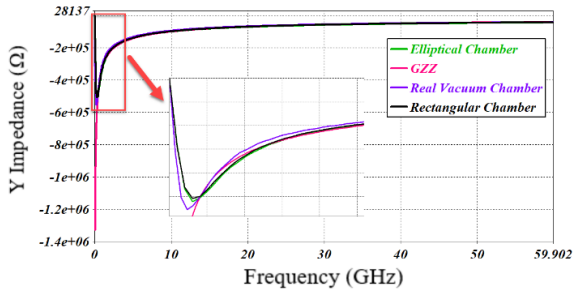

Figure 4: Vertical resistive wall impedance for Figure 1 geometry (violet), GZZ analytical equation (purple), approximated vacuum chamber in rectangular (black) and elliptical (green) geometries.

Transverse results are presented in Figure 3 and 4 where a clear agreement between analytical and simulated results is observed.

It should be noted that for simulation configuration, we employed 2 mm stainless steel walls, normal conducting background, and open boundary in z direction. Also, 1.3 mm bunch length and 20 line per sigma were defined as mesh properties.

Tapers

In the case of tapers, a quick and reliable estimation of the dipolar and quadrupolar impedances in vertical direction is written below [9, 10]:

$$Z_{yD} = -i\frac{\pi}{4}Z_0 w\int_{-\infty}^{\infty}\frac{(g')^2}{g^3}G_1\left(\frac{g}{w}\right)dz \ . \tag{2}$$

$$Z_{yQ} = -Z_{xQ} = -i\frac{\pi}{4}Z_0\int_{-\infty}^{\infty}\frac{(g')^2}{g^2}G_2\left(\frac{g}{w}\right)dz \ . \tag{3}$$

Where

$$G_1(x) = x^3\sum_{m=0}^{\infty}(2m+1)\,\mathrm{csch}^2\phi_m\coth\phi_m \ . \tag{4}$$

$$G_2(x) = x^2\sum_{m=0}^{\infty}(2m+1)\,\mathrm{sech}^2\phi_m\tanh\phi_m \ . \tag{5}$$

g(z) is the vertical gap profile along longitudinal axis, W is the width of the chamber and $\phi_m = (2m+1)\pi x/2$. The best vertical gap profile approximation for tapers was suggested by G. V. Stupakov [11]:

$$g(z) = b_0 + \frac{d}{2}\left(1+\cos\left(\frac{\pi z}{l}\right)\right) \quad |z| < l \tag{6}$$

To compare analytical and simulation results, ILSF typical tapers were simulated in CST Particle Studio (Figure 5 and 6). The separation between tapers is long enough (500 mm) to assure us that the simulation results are length independent [9].

Normal background, electric boundary condition and 2.0 mm bunch length were defined in software configuration. Local mesh settings were added to 20 per line sigma as mesh properties. Therefore, the size of mesh cells was in the order of 0.5 mm.

Loss factor integration was calculated for 7.9 mm, which was the rms bunch length of ILSF storage ring.

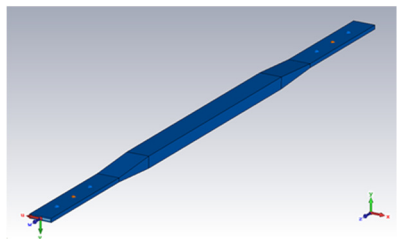

Figure 5: Cavity-like tapers.

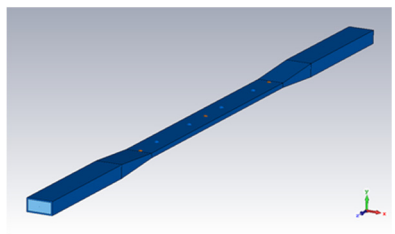

Figure 6: Collimator geometry.

The effect of resistive wall and mesh setting in vertical loss factor can be found in Table 1 in details.

Table 1: A Comparison of Simulation Details in CST Particle Studio for 4.2 mm Gap Size

Method	CST Details	Kick Factor in Y ($\frac{V}{Pc.m}$)
Analytical	-	301.212
CST (Test beam)	PEC (65 million meshes)	294.65
	Stainless steel (65 million meshes)	655.47
CST (Interface for cavity-like structures)	Stainless steel (65 million meshes)	416.83
	Stainless steel (93 million meshes)	412.38
CST (Interface for collimators)	PEC	291.42
	Stainless steel (65 million meshes)	644.81
	Stainless steel (93 million meshes)	651.31

Referring to CST solutions, the impedance of the collimators can only be solved by interface integration method with more mesh number settings. However, finding a reliable number for mesh setting for an accurate impedance calculation was challenging.

Clearly, the impedance is an additive quantity. In addition, the order of components is not critical in impedance calculation. Therefore, we might be allowed to exchange the place of the components in simulation. In collimator case, moving one of the tapers to the other side may convert the collimator to a cavity-like structure. We

ISBN: 978-3-95450-208-0 doi:10.18429/JACoW-IPAC2019-WEPTS101

find out that a well agreement exists between analytical calculations for cavity-like structure, test beam and collimator interface results (Table 1).

Analytical and simulated loss factors are presented in Table 2. The gap size is changed from 4.2 mm to 30 mm. All the components in CST simulations were changed to a cavity-like one. In some cases, the results were verified with interface solution.

Table 2: Loss Factor in Dipole and Quadrupole Impedances

Gap Size [mm]	Dipolar Kick Factor [$\frac{V}{pc.m}$]		Quadrupolar Kick Factor [$\frac{V}{pc.m}$]	
	CST	*Analytical*	*CST*	*Analytical*
4.2	294.65	301.2	27.097	18.87
8.4	54.338	55.3	7.3478	5.709
11.8	16.16	16.3	2.734	2.136
12.2	13.93	13.9	2.415	1.879
25	1.897	1.84	0.567	0.448
30	5.481	5.50	1.854	1.569

Holes

A regular formula for analytical study of the holes can be written as [12, 13]

$$Z_{\parallel} = \frac{jZ_0 k}{6\pi^2}\frac{h^3}{b^2}. \quad (7)$$

$$Z_{\perp} = \frac{j\,2\cos^2\theta}{3\pi^2}\frac{h^3}{b^4}. \quad (8)$$

Based on MAFIA simulations, the validity of this formula is not verified [14]. However, our CST simulations also confirms this fact. The study is done in hole and chamber radii.

Now, the effect of chamber radius is investigated. Table 3 and Table 4 are for $R_{chamber} = 10\ mm$ and $R_{chamber} = 13.5\ mm$, respectively. Apparently, smaller size of the hole radius needs more mesh accuracy. The difference between analytical and simulation results increases by reducing the size of the holes. 1 mm wall thickness was used in this simulations. The comparison was done in $f = 5\ GHz$.

Table 3: Impedance Dependence on the Radius of the Hole (Impedances are in Ω. $R_{chamber} = 10\ mm$)* †

h [mm]	$Z_{Anal\ Longit}$	$Z_{Simul\ Longit}$	$Z_{Anal\ Trans}$	$Z_{Simul\ Transl}$
3	0.10	0.061	0.089	0.089
2	0.026	0.036	0.0162	0.030
1	0.0031	0.0175	0.001	0.007
0.5	6.1e-5	0.0115	3.9e-4	0.002

In comparison with the next table, the effect of chamber radius on calculated impedance could be understood.

As mentioned, the hole approximations in Eq. (7) and (8) are not well matched with simulations.

* Impedances are in Ω.

† The word 'Anal' is refer to analytical results and 'Simul' means simulation one.

Table 4: Impedance Dependence on the Radius of the Hole ($R_{chamber} = 13.5\ mm$) * †

h [mm]	$Z_{Anal\ Longit}$	$Z_{Simul\ Longit}$	$Z_{Anal\ Trans}$	$Z_{Simul\ Trans}$
3	0.058	0.099	0.030	0.061
2	0.015	0.029	0.0054	0.012
1	0.0018	0.014	3.27e-4	≈ 0

M. Takao believes that not considering the effect of current detour from the hole position is the reason of this discrepancy [15]. In addition, the ratio of $Wall\ Thickness/Hole\ Radius$ plays a critical role in this case [16]. For $t/h = 0.3$ the best match between theory and simulation results is going to happen. In more or less wall thicknesses, results will be mismatched. Apparently, it seems that the effect of wall thickness has not been completely covered in the hole impedance theories.

Rectangular Grooves

A complete set of equations can be presented here [17, 18]

$$Z(\omega) = -i\,\omega\frac{Z_0}{2\pi bc}\left(gh - \frac{g^2}{2\pi}\right) \quad (9)$$

$$Z(\omega) = -i\,\omega\frac{Z_0 h^2}{2\pi^2 bc}\left(2\ln\left(\frac{2\pi g}{h}\right)+1\right) \quad (10)$$

$$Z(\omega) = -i\,\omega\frac{Z_0 h^2}{4\pi^2 bc}\left(2\ln\left(\frac{2\pi b}{h}\right)+1\right) \quad (11)$$

A rectangular step was simulated around a circular chamber to verify analytical estimations (Figure 7). g is 1 mm and the diameter of vacuum chamber is $b = 10\ mm$.

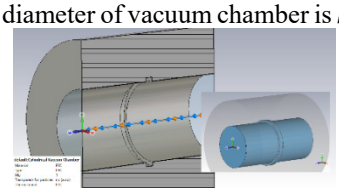

Figure 7: A typical flange gap in a circular vacuum pipe.

For all different depths of the rectangular groove, Eq.(9) is applied in the case of $g \le h$, Eq. (10) for $g \gg h$ and Eq. (11) for $g \sim b, h \ll b$. The results are presented in Table 5.

Table 5: Impedance Study of the Rectangular Groove Height from the Analytical and Simulation Point of View.

Height of Gap	$Z_{Analytical}(\Omega)$	$Z_{Simulation}(\Omega)$
$h = 1\ mm$	0.856	0.871
$h = 4\ mm$	4.627	4.47
$h = 5\ mm$	5.884	5.729
$h = 10\ mm$	12.167	15.165

CONCLUSION

Analytical results in resistive walls, rectangular steps and tapers are in well agreement with simulation results. Therefore, for these components, beam dynamic calculations can be done based on analytical equations.

ISBN: 978-3-95450-208-0 doi:10.18429/JACoW-IPAC2019-WEPTS101

REFERENCES

[1] Khosravi, N. *et al*., "Impedance Study of resistive walls at Iranian light Source Facility," in *3rd Iranian particle accelerators conference.* 2017: Isfahan University of Technology, Isfahan, Iran, 2017.

[2] Khosravi, N. *et al*., "Impedance and Wakefield study of Vacuum Flanges at ILSF Storage Ring," in *3rd Iranian particle accelerators conference.* 2017: Isfahan University of Technology, Isfahan, Iran, 2017.

[3] Shafiee, M. *et al*., "Design and Development of Configurable BPM Readout System for ILSF." 2016.

[4] Shafiee, M., H. Behnamian, and S. Feghhi, "A study of wake potentials for the pick-ups in storage ring." *Journal of Instrumentation*, 2017. **12**(12): p. T12006.

[5] Shafiee, M., S. Feghhi, and J. Rahighi, "Experimental performance evaluation of ILSF BPM data acquisition system." *Measurement*, 2017. **100**: p. 205-212.

[6] Khosravi, N. *et al*., "Impedance and collective effect Studies at ILSF Storage Ring," in *10th ILSF Users' Meeting*. 2018: Qazvin, Iran.

[7] Gluckstern, R.L., J. van Zeijts, and B. Zotter, "Coupling impedance of beam pipes of general cross section." *Physical Review E*, 1993. **47**(1): p. 656.

[8] Smaluk, V. *et al*., "Beam-based model of broad-band impedance of the Diamond Light Source." *Physical Review Special Topics-Accelerators and Beams*, 2015. **18**(6): p. 064401.

[9] Smaluk, V. *et al.*, "Coupling impedance of an in-vacuum undulator: Measurement, simulation, and analytical estimation." *Physical Review Special Topics-Accelerators and Beams*, 2014. **17**(7): p. 074402.

[10] Stupakov, G., "Low frequency impedance of tapered transitions with arbitrary cross sections." *Physical Review Special Topics-Accelerators and Beams*, 2007. **10**(9): p. 094401.

[11] Stupakov, G., "Geometrical wake of a smooth taper." *Part. Accel.*, 1995. 56(SLAC-PUB-7086): p. 83-97.

[12] Kurennoy, S., "Pumping slots: coupling impedance calculations and estimates." 1993, Superconducting Super Collider Lab., Dallas, TX (United States).

[13] Gluckstern, R., "Coupling Impedance of a Hole in a Thick Wall Beam Pipe." CERN SL/91 (AP), 1991.

[14] Thiagarajan, V. *et al*., "Calculation of the coupling impedances of holes and slots on the liner using MAFIA and scaling." 1993, Superconducting Super Collider Lab., Dallas, TX (United States).

[15] Takao, M., T. Higo, and K. Bane, "Estimation of the longitudinal impedance of the ATF damping ring." 1992, National Laboratory for High Energy Physics.

[16] Gluckstern, R.L., "Coupling impedance of a single hole in a thick-wall beam pipe." *Physical Review A*, 1992. **46**(2): p. 1106.

[17] Kurennoy, S. and S. Purtov, Coupling impedance for an inhomogeneity of accelerator vacuum chamber. Part. Accel., 1990. **36**(IHEP-90-31): p. 223-240.

[18] Kurennoy, S. and G. Stupakov," A new method for calculation of low-frequency coupling impedance." Part. Accel., 1993. **45**(SSCL-P-332): p. 95-110.